AIAA The World's Forum for Aerospace Leadership Purchased from American Institute of Aeronautics and Astronautics

Chapter 17

Assessment of Thrust Chamber Performance

Douglas E. Coats*
Software and Engineering Associates, Inc., Carson City, Nevada

Nomenclature

A = cross-sectional area
C^* = characteristic velocity, $p_c A^*/\dot{m}$
Isp = specific impulse, $F/\dot{m}$
F = thrust
M = Mach number
$\dot{m}$ = mass flow rate
O/F = propellant mixture ratio
p = pressure
r = nozzle radius
Re = Reynolds number
y = distance from the nozzle wall

Greek

α = nozzle wall angle
δ = boundary-layer thickness
δ^* = boundary-layer displacement thickness
γ = ratio of specific heats, Cp/Cv
ε = expansion ratio (A_e/A^*)
η = efficiency
θ = boundary-layer momentum thickness, also nozzle half-angle

Subscripts

a = ambient
c = chamber

Copyright © 2004 by Douglas E. Coats. Published by the American Institute of Aeronautics and Astronautics, Inc., with permission.

*President. Associate Fellow AIAA.

AIAA The World's Forum for Aerospace Leadership Purchased from American Institute of Aeronautics and Astronautics

div = divergence
e = nozzle exit
eq = chemical equilibrium
f = finite contraction ratio
froz = chemically frozen
i = ith zone or striation
kin = finite rate chemistry
th = theoretical or ideal
xz = interzonal
∞ = infinite contraction ratio
0 = stagnation, Eq. (1)

Superscripts

$*$ = nozzle throat plane

I. Introduction

THE assessment of thrust chamber performance is not a new topic, and there are many excellent sources of information on it. In the United States the reports of Pieper[1] and Evens[2] address all of the issues discussed in this chapter. The works of Sutton,[3] and Zucrow and Hoffman[4] cover many of the topics in detail.

Liquid propellant rocket engines (LREs) are devices that convert the latent energy of the propellants into sensible heat in the combustion chamber and then convert it again into kinetic energy in the nozzle. To make comparisons between different engine and system designs, we must be able to assess the performance of the LRE. The thrust chamber of an LRE produces the measurable output of a liquid propellant powered rocket, i.e., thrust, and hence the assessment of its performance is of great importance in evaluating the overall performance of the entire system. Because of the tremendous energy flow in LREs, these engines are characterized by small performance losses because of heat loss, friction, vaporization, and mixing inefficiencies. Even small losses, however, have a large impact on delivered payload or on range of the system and are therefore important.

To assess the performance of a system, one must establish a figure of merit that characterizes the system. The figure of merit must also be a measurable quantity. The most used such quantity for LRE thrust chambers is the specific impulse *Isp*. The specific impulse is defined as the engine thrust divided by the mass flow rate of the propellants, and thus it tells us how effectively the thrust chamber converts propellant into thrust. The specific impulses delivered to vacuum and to ambient pressure conditions are both commonly used.

Although performance as measured by specific impulse is important, the design of a thrust chamber is quite often driven by other factors, including weight, power extraction, physical packaging constraints, materials and life cycle, heat transfer/cooling, combustion stability considerations, environmental and safety concerns, and propellant shelf life. To describe methods of assessing thrust chamber performance, we shall first discuss how to estimate the maximum possible performance obtainable, and then the losses experienced by real engines

AIAA The World's Forum for Aerospace Leadership Purchased from American Institute of Aeronautics and Astronautics

and the elements required to model these losses. Specific requirements for modeling these losses are then addressed. Also discussed are those phenomena that are not well characterized and hence lack adequate analytical models to describe them. Finally, descriptions of specific codes and procedures in use in the United States are presented.

II. Definition of Ideal or Theoretical Performance

Maximum performance of a thrust chamber, sometimes called ideal or theoretical performance, is achieved if the propellants entering the thrust chamber react completely and chemical equilibrium is maintained throughout the expansion process. Additionally, the flow should be isentropic and one-dimensional. Under these ideal conditions, the thrust chamber performance is dependent on the physical, chemical, and thermodynamic properties of the propellants and their combustion products, and on the operating conditions of the engine, that is, propellant mixture ratio O/F, chamber pressure p_c, expansion ratio ε, and ambient pressure p_a. For the ideal thrust chamber, we neglect real-world design parameters, such as nozzle geometry, size, injector element design, engine coolant configuration, and baffles.

Even with such a seemingly simple definition of ideal performance, a certain amount of disagreement can occur. For example, the value of the total pressure to be used for the expansion process depends on the assumption of either an infinite or a finite contraction ratio for the combustion chamber. From simple one-dimensional relationships, the ratio of these two total pressures can be approximated as

$$p_{0f}/p_{0\infty} = \frac{\left[1 + \dfrac{(\gamma - 1)}{2} M_f^2\right]^{\gamma/(\gamma-1)}}{1 + \gamma M_f^2} \approx 1 - \frac{\gamma}{2} M_f^2 \tag{1}$$

The decrease in total pressure due to accelerating the flow affects primarily the mass flow rate of the nozzle. However, when computing the performance delivered to ambient pressure, there is a small decrease in performance due to the $p_a/\dot{m}$ effect.

Thus, our theoretical maximum performance is defined as an isentropic one-dimensional flow in chemical equilibrium (often called shifting equilibrium) at the thrust chamber O/F and chamber pressure (infinite or finite contraction ratio). More information on the chemical equilibrium solutions to this problem is given by Gordon and McBride.[5,6]

III. Real Engine Losses

We have broken down the deviations from ideal performance into two classes of real engine losses: those that are well characterized and those that are not. Such a breakdown is very subjective and really just rates our confidence level in our understanding of the phenomena. Included in the well-characterized losses are the boundary-layer and heat transfer losses, finite rate chemical kinetics losses, and divergence or two-dimensional losses. The poorly characterized losses

AIAA The World's Forum for Aerospace Leadership Purchased from American Institute of Aeronautics and Astronautics

include the injection, atomization, vaporization, and mixing processes in the combustion chamber.

A. Well-Characterized Losses

1. Boundary-Layer Loss

Propulsive LREs are generally characterized by high Reynolds number flow. Table 1 lists the Reynolds numbers based on throat conditions for a variety of engines. Because the mass flux is highest in the throat region, the throat Reynolds number is almost always the largest encountered during the nozzle expansion. Other characteristics of importance in LREs that affect boundary layers are the methods of wall cooling. Because the enthalpy of the combustion products is very high, the chamber and nozzle walls need to be protected. Some standard ways of protecting the walls include regenerative cooling, barrier or film cooling, radiation cooling, ablative walls, and slot injection or transpiration cooling. A high Reynolds number means that the viscous layer next to the wall is very thin, which in turn indicates that the classical thin shear or boundary-layer assumptions are valid. Hence, except for the smallest engines, the core flow in the engine can be treated as inviscid, and the solution of the wall shear layer can be uncoupled from the core flow. The true singular perturbation nature of the boundary-layer equations becomes quite apparent in rocket engine flows, because the outer or core flow is not uniform and can vary significantly in the radial direction over the distance of a boundary-layer thickness. In addition, when film cooling is used in the engine, there is a significant total enthalpy gradient near the wall, and hence the outer flow can be highly rotational. The standard simplistic ways of looking at the boundary-layer thicknesses can be very misleading, and questions about the quantity of mass flow in the boundary layer have limited meaning.

Because solution procedures for the boundary-layer equations are well established, the only real questions are what physical phenomena are important and how best to model them. Smaller engines tend to have laminar boundary layers, whereas the larger engines are almost always turbulent. One rule is that engines with less than 45,000 N (10,000 lbf) thrust are laminar. A slightly

Table 1 Nozzle characteristics for various engines

Engine	Thrust, 10^3 N	p_c, bars	r^*, mm	ε	Re_{r^*}
Hughes 5 lbf	0.111	1.72	2.37	296.6	1.10×10^4
NASA/LeRC Hi-E	2.40	24.82	12.7	1025	1.73×10^5
XLR-134	2.28	35.16	10.06	767.9	1.80×10^5
STS/RCS	3.84	10.34	25.93	28.46	1.75×10^5
Advanced Space Engine	100.67	157.68	31.85	400.7	2.20×10^6
RL 10	60.05	27.19	65.28	205.03	1.29×10^6
RD-170	7915.73	244.65	117.75	36.9	1.62×10^7
SSME	2062.45	226.49	130.88	77.5	1.18×10^7
F1	7786.55	68.4	444.5	15.76	1.81×10^7

AIAA The World's Forum for Aerospace Leadership Purchased from American Institute of Aeronautics and Astronautics

more appealing transition criterion is that transition occurs when the Reynolds number, based on the boundary-layer momentum thickness Re_θ, exceeds 360. Because most engines are high-thrust engines, one of the first choices to be made is the selection of the turbulence model. Coats et al.[7] have estimated that the maximum calculated variation in boundary-layer loss results is approximately 25% when a κ-ε turbulence model is compared to an algebraic eddy viscosity (e.g., Cebeci and Smith[8]) model. Because the boundary loss is usually on the order of 1–2% and almost never more than 4% of the total performance, the variation of calculated loss with turbulence model will be in the range of 0.25–1% of the total performance. Without high quality experimental data to validate turbulence models for rocket engine flows, there is no way of knowing which of the available turbulence models should be used.

Other questions arise as to which chemistry model should be used in the boundary-layer calculation. For most simple flows, i.e., single O/F core flows, almost any chemistry model will give results within the known accuracy range of the boundary-layer equations. Once higher fidelity core flow models are used, however, at least a variable gas properties treatment should be used in the boundary-layer model. If heat transfer results are required in addition to performance losses, then the choice of chemistry model can be quite important. For example, the adiabatic wall temperature at the nozzle exit plane for the Vulcain engine is 350 K greater for the finite rate calculation than for a chemical equilibrium calculation, an important difference if you are determining the cooling requirements of the engine! Another consideration in selecting the boundary-layer chemistry model is the need to predict what happens to turbine exhaust gases that are injected into the engine downstream of the throat. These injected gases have a pronounced effect on the boundary-layer profiles, as shown in Fig. 1, and can lead to either endothermic or exothermic reactions. Transpiration cooling modeling requirements will also have an impact on the chemistry model selection.

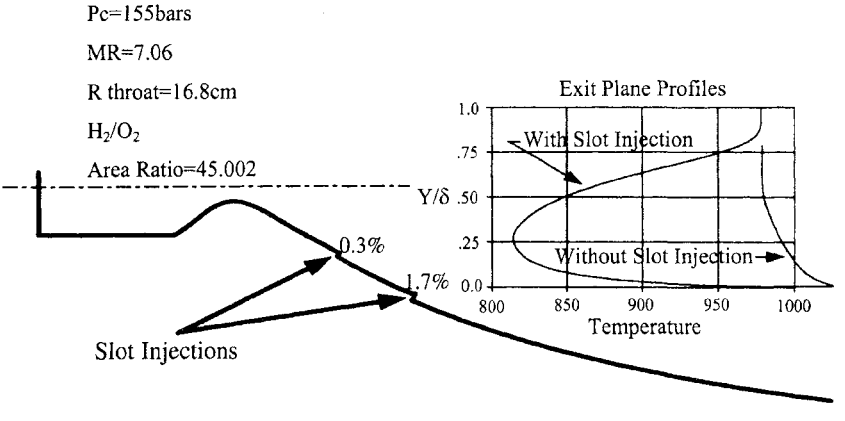

Fig. 1 Boundary-layer profile with tangential slot injection.

AIAA The World's Forum for Aerospace Leadership Purchased from American Institute of Aeronautics and Astronautics

2. *Divergence*

The divergence or two-dimensional loss is conceptually the simplest of all of the losses. The velocity vectors of the gases exiting the nozzle are not necessarily aligned with the axis of the nozzle or vehicle. The result of the misalignment is that not all of the kinetic energy of the flow results in axial thrust. This loss is mainly a function of the nozzle geometry, and to a lesser extent of the ratio of specific heats γ.

It is generally agreed that there is little coupling between the finite rate chemical kinetics and the two-dimensional flowfield. Furthermore, except for the smallest engines or very large area ratio nozzles, the wall boundary layer is very thin and interacts with the core flow only to second order. Other performance loss considerations are due to the formation of shock waves, large gradients in the flow due to O/F striations, two-phase flow due to poor vaporization of droplets, and large sources of rotationality due to geometric or engine/injector phenomena.

For most well-designed engines these considerations are not applicable. Hence, the divergence loss can be adequately modeled by a variable gas properties solution to the full Euler equations. However, solutions to these equations, although isoenergetic along streamlines, do allow for shock waves and variations in the total enthalpy of the flow, and thus can be used for off-design analysis.

One last consideration is that the sonic line or surface in the nozzle throat region is not flat but curved. The result of this curvature is that there is less mass flow through the nozzle than would be predicted by one-dimensional flow analysis. The series solution by Hall,[9] modified by Kliegel and Levine,[10] gives a good estimate of the nozzle discharge coefficient.

3. *Finite Rate Kinetics*

When highly energetic propellants are burned in the combustion chamber, the resulting high temperatures cause many of the normally stable molecules to dissociate. During the subsequent expansion in the nozzle, the kinetic rate process tends to recombine these molecules, making sensible heat available to further drive the expansion. Most notably, it is the recombination of hydrogen molecules to form H_2, and the formation of CO_2 from CO and O, which release the bulk of the energy. The short residence time in the nozzle, coupled with rapidly decreasing pressure and temperature, do not allow the flow to stay in chemical equilibrium (maximum heat release).

For most propellant systems, the reaction rate mechanisms and their associated rate data are reasonably well understood. The rate data are usually known within an order of magnitude, which is adequate for determining the finite rate kinetics loss. There are several ways in which this loss is expressed. The two most common are the ratio of specific impulse with and without the loss, η_{kin}, and the fraction of the difference between equilibrium and frozen flow, η'_{kin}:

$$\eta_{\text{kin}} = Isp_{\text{kin}}/Isp_{\text{eq}} \tag{2a}$$

$$\eta'_{\text{kin}} = (Isp_{\text{kin}} - Isp_{\text{froz}})/(Isp_{\text{eq}} - Isp_{\text{froz}}) \tag{2b}$$

AIAA The World's Forum for Aerospace Leadership Purchased from American Institute of Aeronautics and Astronautics

The loss is mainly a function of the propellant system, chamber pressure, and residence time in the nozzle. High-pressure systems tend to have smaller losses, because of the large number of molecular collisions. The nozzle length scale is also an important parameter in that it sets the residence time in the nozzle. Although high-area-ratio nozzles tend to have larger losses, this effect is less important than the other factors discussed. Table 2 shows some typical values for the kinetic loss efficiencies. As can be seen from table, amine fueled (e.g., hydrazine, UDMH, MMH) engines usually exhibit low kinetic efficiencies.

Another consideration is the starting point for the expansion. If the species in the combustion chamber do not start out in a state near chemical equilibrium, then there is the potential that they will not approach equilibrium within the nozzle. The nonequilibrium starting condition problem is especially important at off-optimum mixture ratios.

4. Radiation

Energy can escape the thrust chamber in the form of radiation. The foremost methods are from the combustion chamber walls and the nozzle, and from the hot gases. The first two losses are usually coupled with the boundary-layer loss, while the second is generally small. The majority of the energy radiated from the hot gases is in the form of infrared radiation. The largest common emitters of infrared radiation are CO, CO_2, and H_2O. These molecules emit at discrete spectral lines, and black or gray body radiation treatments are inappropriate. The majority of the radiation emitted by these species is transferred to the walls or is reabsorbed by the gases. Only a small fraction of the energy escapes out of the nozzle. In terms of the overall energy flow rate, the loss out of the nozzle is insignificant. However, for radiation-cooled nozzles the performance loss should be treated as a boundary condition for the boundary-layer calculation. Non-performance-related applications in which radiation can be the dominant effect include base heating and exhaust plume signatures.

B. Poorly Characterized Losses, the Energy Release Efficiency

The purpose of an injector element in the thrust chamber is to introduce the fuel or oxidizer in such a way that both components mix and combust completely. There are many different injector types, and the fuel and oxidizers may be

Table 2 Kinetic loss ratios

Engine	Propellants	η'_{kin}
F-1	LOX/RP-1	0.98
Atlas Booster	LOX/RP-1	0.90
Atlas Sustainer	LOX/RP-1	0.90
TR201	NTO/A50	0.50
R-4D	NTO/MMH	0.30
Titan III (Stage I)	NTO/A50	0.75

AIAA The World's Forum for Aerospace Leadership Purchased from American Institute of Aeronautics and Astronautics

injected as gas-gas, liquid-gas, gas-liquid, and liquid-liquid. Each method of injection has its own advantages and associated problems. To illustrate the sources of potential losses, we will concentrate on liquid-liquid injection.

The process of injection, atomization, vaporization, combustion, and mixing is reminiscent of turbulence in fluid flow. That is, there are a great many length scales that must be resolved to characterize the problem. First, the liquid stream of fuel or oxidizer experiences an instability that causes it to start to break up. Prior to, during, or after breakup, the stream can collide with another stream. The original breakup is called primary atomization, and breakup of the larger drops is referred to as secondary atomization. The processes associated with secondary atomization include the dynamic stability of the droplets and collisions among droplets. Finally, the droplets vaporize in the presence of the hot combustion gases. In the case of supercritical combustion, the problems are less well understood.

Liquid rocket engines do not always vaporize all of the propellants within the combustion chamber. In many engines using hydrocarbon fuels, the fuel tends to vaporize much more slowly than the oxidizer (fuel-controlled burning). This slow vaporization can cause a large shift between the injected O/F and the effective gas-phase O/F at the exit of the combustion chamber. Engine designers often trade combustion chamber length and ease of injector fabrication for vaporization efficiency.

One of the well-known characteristics of dense sprays is that they do not behave like collections of individual droplets. Incomplete vaporization and poor mixing of the vaporized propellants can cause significant losses in performance. Many people think that of the two, the mixing loss is much larger than the vaporization loss. This type of mixing loss is sometimes referred to as cluster effect, fine mixing, intrazonal mixing, or micromixing, as compared with coarse mixing, which is discussed next.

The thrust chamber walls are sometimes cooled by injecting a fuel (or oxidizer) film spray on the wall. The lower (or higher) O/F in this region reduces the flame temperature, and thus the heat transfer rate. Because these propellants do not combust in a way that releases the maximum amount of heat, there is a loss associated with this process, as compared with our theoretical performance at the overall engine mixture ratio. This loss is referred to as coarse mixing, interzonal mixing, or macromixing loss.

Of the two mixing losses, the interzonal is the easiest to conceptualize because it is part of the engine design and the percentage of fuel near the wall is known. Figure 2 illustrates the amount of noncombusted fuel required to produce the 2.5% loss that is typical of many engines. These results, which are from equilibrium calculations for an RP-1/LOX system and an NTO/UDMH system, show that approximately 25% of the RP-1 and 35% of the UDMH would have to be unburned in order to reduce the *Isp* by 2.5% from its maximum value.

Sometimes, all of the above losses are lumped together and referred to as combustion efficiency or energy release losses. The most direct measurement that we have of these losses is the measured C^* efficiency of the engine. If the C^* efficiency is used to back out this loss, then the effect of the nozzle discharge

AIAA The World's Forum for Aerospace Leadership Purchased from American Institute of Aeronautics and Astronautics

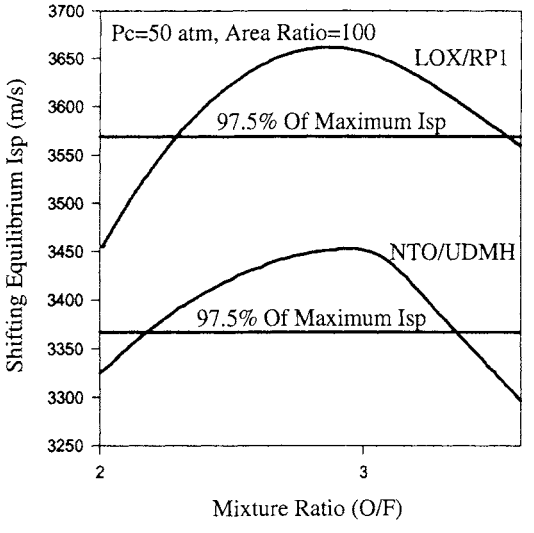

Fig. 2 Vacuum *Isp* variation with mixture ratio.

coefficient C_D must be subtracted out. In the absence of any losses, the C^* efficiency η_{C^*} is

$$\eta_{C^*} = 1/C_D \tag{3}$$

Note that the C^* efficiency is not the same as combustion efficiency, although they are very close for most engines and propellant systems.

IV. Modeling

Analytical modeling of thrust chamber performance encompasses a wide range of approaches. It can apply to anything from using the isentropic perfect gas relations to a full Navier–Stokes (FNS) simulation. The information to be derived from the modeling drives the complexity of the selected model. For example, a value of 91% of the theoretical *Isp* provides a reasonable prediction of performance. It does not, however, provide any information on how the losses occurred or how they could be reduced. Another important point is that the model output is no better than the quality of the input data.

In this section we will explore a variety of modeling approaches, try to assess the accuracy of the approaches, and make some recommendations. Starting first with the calculation of ideal performance, we will cover the well-characterized losses and then cover the approaches to modeling the poorly characterized losses.

Three types of modeling will be discussed: simple modeling, moderately complex modeling, and complex modeling. In the first category, very simple relations will be used to estimate the magnitude of each loss, i.e., Eq. (2). For

AIAA The World's Forum for Aerospace Leadership Purchased from American Institute of Aeronautics and Astronautics

the moderate category, fairly sophisticated models are used to calculate each loss. In the final category, all (or at least most) of the losses are modeled in a coupled manner.

One point should be made with respect to the calculation of the performance of a thrust chamber; this is simply that *Isp* is a wonderful quantity in its insensitivity to uncertainty. If, when modeling an engine, the energy of the propellants is correctly specified and the conservation of mass, energy, and momentum is achieved to reasonable accuracy, then the answer will be almost independent of the small variations in modeling assumptions. On the other hand, there are those who seek accuracies of within a few tenths of a percent.

A. Ideal or Theoretical Performance

The calculation of thrust chamber performance, assuming chemical equilibrium with complex products of combustion, is now easily accomplished.[6] Recent controversies aside, there are a number of chemical equilibrium codes available that give the same answers to the known accuracy of the thermodynamic data. Only two thermodynamic states and the elemental composition are required to fully determine the state of chemical equilibrium. The usual assumptions made are that the composition and enthalpy (heat of formation plus sensible heat) of the propellants are known. The enthalpy of the propellants in the tank is often used if known; otherwise the enthalpy at the normal boiling point (NBP) is a good choice. The chamber pressure is assumed and an enthalpy-pressure (HP) solution is found. The products of combustion are then expanded to different pressures using the entropy of the products (PS) in the chamber to close the set. From the conservation of mass and energy, the area ratios and velocities can be found at each solution point. As stated earlier, the differences between finite area and infinite area combustion are minimal, and Eq. (1) can be used to apply the correction to the chamber pressure.

One-dimensional chemical equilibrium solutions are among the most useful modeling tools available. Not only do they give us the theoretical maximum performance, but they also allow us to explore the effects of modifying propellant formulations and mixture ratios, with a minimal expenditure of time and effort.

B. Well-Characterized Losses

Earlier in this chapter we discussed the well-characterized losses and indicated some of the more important features of these losses. Now we will concentrate on methods of solutions, the required input for the solutions, and the potential accuracy of the modeling approach. It should always be remembered that the accuracy of a solution is dependent not only on the correctness of the model but also on the accuracy of the input data. There is no advantage in using complicated models if the input required is not known to reasonable accuracy. Such approaches mask the uncertainty of the answers and are often misleading.

To this point we have not formally addressed the interactions of the various loss mechanisms. Obviously, almost every mechanism in the combustion and flow process affects every other mechanism to some extent. As we pointed out, however, for high Reynolds number flows, the boundary layer and core flow can be decoupled. These are not the only losses that can be uncoupled. Table 3,

AIAA The World's Forum for Aerospace Leadership Purchased from American Institute of Aeronautics and Astronautics

Table 3 Interaction of physical phenomena with performance loss calculations (from Ref. 1)

Phenomena	Divergence loss	Boundary-layer loss	Finite rate kinetics loss	O/F Maldistribution loss	Energy release loss
Non-one-dimensional flow	——	1st order,[a] >0.2%	2nd order,[b] <0.2%	Not Imp.[c]	Not Imp.
Viscous and heat transfer	Not imp.	——	Not imp.	Not imp.	Not imp.
Finite rate chemistry	Not imp.	2nd order, <0.2%	——	Not imp.	Not imp.
Nonuniform mixture ratio	Not imp.	1st order, >0.2%	1st order, >0.2%	——	Not imp.
Incomplete energy release	Not imp.	2nd order, <0.2%	1st order, >0.2%	Not imp.	——

[a]1st order, >0.2% = primary importance (could be >0.2% on *Isp*).
[b]2nd order, <0.2% = secondary importance (probably <0.2% on *Isp*).
[c]Not imp. = generally not important.

AIAA The World's Forum for Aerospace Leadership Purchased from American Institute of Aeronautics and Astronautics

which was taken from Ref. 1, shows the estimated coupling between loss mechanisms in LREs. This uncoupling of losses is very important for simple and intermediately complex modeling.

For all but the most complex of modeling approaches, the most common method is to separate the individual losses and treat them as efficiencies η or decrements Δ to the theoretical *Isp*. That is,

$$Isp_D = Isp_{\text{th}} \cdot \prod_i \eta_i \tag{4a}$$

or

$$Isp_D = Isp_{\text{th}} - \sum_i \Delta Isp_i \tag{4b}$$

Although both approaches have their ardent supporters, there are really no significant differences between the two. In addition to its simplicity, the separation approach has the extra advantage that it identifies both the sources and magnitudes of the losses.

1. Boundary-Layer Loss

Before proceeding into actual methods of modeling the boundary-layer loss, the coupling of regenerative heat transfer with the theoretical specific impulse must be established. For performance prediction in most regeneratively cooled engines, it is quite acceptable to model the nozzle wall as adiabatic and the propellants at their tank enthalpies, because the energy transferred to the wall is put back into the fuel. If the nozzle wall is modeled as a cold wall, however, then the enthalpy of the incoming fuel must be adjusted upward by the amount of heat extracted. This observation is particularly important when the modeler is using some measured data. For example, if measured fuel and oxidizer inlet temperatures are used to establish the enthalpies of the propellants, the cold wall heat transfer model must be used. Otherwise, the predicted thrust chamber performance will be much too high.

Simple equations for predicting the nozzle boundary-layer loss have for the most part not been very successful. Our recommendation is that simple empirical equations not be used unless the user has a great deal of experience with the specific engine. Although engine-specific empiricism is acceptable, simplified general empiricism does not work well for the boundary-layer loss.

Part of our reluctance to endorse any general empirical relation is that boundary-layer codes have become so easy and inexpensive to use. Integral method codes, such as the TBL[11] code, have been available for decades and have a significant amount of rocket engine empiricism built into them. Modern boundary-layer codes using finite difference are now robust and easy to use. Computer codes based on parabolized and full Navier–Stokes equations are also available to compute the wall shear layer loss.

AIAA The World's Forum for Aerospace Leadership Purchased from American Institute of Aeronautics and Astronautics

Considering the state of our knowledge in turbulence modeling for rocket engine flows, variable gas properties boundary-layer codes are adequate for performance prediction loss modeling. However, if the boundary-layer results will also be used for wall heat transfer calculations, then chemistry modeling should also be included.

2. *Divergence*

For a simplified approach to divergence loss, the loss expression given in Eq. (5) can be used:

$$\eta_{\text{div}} = (1 + \cos\theta)/2 \tag{5}$$

where θ is the cone half-angle (or average nozzle expansion angle). This expression was derived for conical nozzles and its development is presented in Zucrow and Hoffman.[4] Figure 3 illustrates the nomenclature.

Euler solvers are recommended for the moderately complex modeling approach because the divergence loss is essentially an inviscid phenomenon. There are many perfect gas and variable properties programs to choose from. Both the method of characteristics (MOC) and fixed grid finite difference or finite volume solvers are entirely adequate for determining the two-dimensional or divergence loss in most propulsive nozzles of interest. Although steady-state MOC solvers are fast and very accurate, they require a supersonic start line to begin their solution. This requirement means that some other method is needed to generate the transonic solution. Also, most MOC solvers can handle only weak shock waves. The latter condition is usually met in most propulsive nozzles of interest.

However, for very small nozzles or systems with large mixture ratio distributions, more complex codes are recommended. When the boundary layer starts to engulf a significant fraction of the nozzle flow, the use of parabolized or full Navier–Stokes (PNS or FNS) solvers is indicated. These types of codes should be used at least once in the analysis process to ensure that the simpler solvers are doing an adequate job. For systems with large O/F gradients, chemistry should be incorporated into the models. At least an equilibrium chemistry

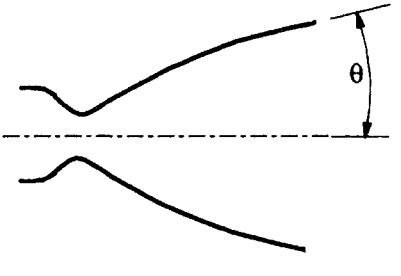

Fig. 3 Simplified nozzle divergence efficiency.

AIAA The World's Forum for Aerospace Leadership Purchased from American Institute of Aeronautics and Astronautics

Euler solver is required and a finite rate chemistry solver is preferred. Finite rate chemistry Euler solvers have been available for almost three decades.[12]

The magnitude of the divergence loss is around 2%. For systems without large O/F gradients or very thick boundary layers, good Euler solvers are probably accurate to within 5% of the divergence loss or 0.1% of the *Isp* loss. Because they tend to use coarser grids than Euler solvers, PNS and FNS solvers are not quite as accurate, and the error is estimated to be 10–15%. PNS codes are less likely to suffer from this problem than FNS codes, because they can be run at higher spatial resolutions. Another problem with higher fidelity models is that the input data are not known to the same order of accuracy of the models. Kushida et al.[13] have reported very good agreement between predictions and measured data when using an MOC/boundary layer method for a very small high area ratio thruster, the Hughes 5 lbf engine in Table 1. The computed boundary-layer thickness for that nozzle was 28% of the radius at the nozzle exit plane.

3. *Finite Rate Kinetics*

For most systems, the finite rate kinetics loss is less than 2%. Hence, simply assuming a constant value for η'_{kin} of 0.66 will suffice for most systems. There are many systems, however, in which this approximation is very poor, most notably, low pressure amine and fluorinated systems. In the absence of data about a particular system, the minimum acceptable model is a one-dimensional finite rate kinetics calculation. Arrhenius rates are known within an order of magnitude for most of the important reactions in chemical systems of current interest. The difference in calculated kinetics loss between one- and two-dimensional solutions is usually very small. Because we have recommended the use of chemistry models for the divergence loss to handle striations in the flow, however, the use of an Euler solver with finite rate kinetics capability is also recommended.

Although PNS solutions with finite rate kinetics can be achieved in somewhat reasonable computational times, adding kinetics to FNS solutions results in very long execution times for rather poorly resolved spatial meshes. Under normal conditions, we do not recommend the use of FNS solvers to calculate the kinetics loss.

The rates chosen for these calculations have an obvious impact on the magnitude of the loss. In the United States, the rates shown in Table 4 are recommended for CHON systems in the two-dimensional kinetics (TDK) code documentation,[14] with the rate data taken from Baulch et al.[15–17] and Jensen and Jones.[18] The chemical reactions considered are between the species, CO, CO_2, H, H_2, H_2O, N, NO, N_2, O, OH, and O in initial chemical equilibrium. Recommended third body efficiencies for various species are shown in Table 5. Perturbing the H+H and CO+O recombination rates by a factor of 30 downward has the effect on kinetic efficiency shown in Table 6 for an engine with a nozzle expansion ratio of 100, NTO/A50 propellants at a stoichiometric mixture ratio, and a chamber pressure of 7 atm. As can be seen from the table, the changes in performance are minimal.

AIAA The World's Forum for Aerospace Leadership Purchased from American Institute of Aeronautics and Astronautics

Table 4 Reaction rate data for the CHON system

Reactions	A[a]	N	B	Meas., M	Reference
$H + H + M = H_2 + M$	6.4E17	1.0	0.0	Ar	Baulch[15] 30U
$H + OH + M = H_2O + M$	8.4E21	2.0	0.0	Ar	Baulch[15] 10U
$O + O + M = O_2 + M$	1.9E13	0.0	−1.79	Ar	Baulch[15] 10U
$N + O + M = NO + M$	6.4E16	0.5	0.0	N2	Baulch[17] 10U
$N + N + M = N_2 + M$	3.0E14	0.0	−0.99	N2	Baulch[17] 10U
$CO + O + M = CO_2 + M$	1.0E14	0.0	0.0	Ar	Baulch[16] 30U
$O + H + M = OH + M$	3.62E18	1.0	0.0	Ar	Jensen[18] 30U
$O_2 + H = O + OH$	2.2E14	0.0	16.8		Baulch[15] 1.5U
$H_2 + O = H + OH$	1.8E10	−1.0	8.9		Baulch[15] 1.5U
$H_2 + OH = H_2O + H$	2.2E13	0.0	5.15		Baulch[15] 2U
$OH + OH = H_2O + O$	6.3E12	0.0	1.0		Baulch[15] 3U
$CO + OH = CO_2 + H$	1.5E7	−1.3	−0.765		Baulch[15] 3U
$N_2 + O = NO + N$	7.6E13	0.0	75.5		Baulch[17] 3U
$O_2 + N = NO + O$	6.4E9	−1.0	6.25		Baulch[17] 2U
$CO + O = CO$	2.5E6	0.0	3.18		Baulch[16] 2U
$CO_2 + O = CO + O$	1.7E13	0.0	52.7		Baulch[16] 3U

[a] $k = AT^{-N} \exp(-1000B/RT)$, in units of cc, K, mole, s.

AIAA The World's Forum for Aerospace Leadership Purchased from American Institute of Aeronautics and Astronautics

Table 5 Third body recombination efficiency ratio (CHON system), as recommended by Kushida[19]

Species	H + H	H + OH	O + O	N + O	N + N	CO + O	O + H
Ar	1.0	1.0	1.0	0.8	1.0	1.0	1.0
CO	1.5	3.0	4.0	1.0	1.0	1.0	4.0
CO_2	6.4	4.0	8.0	3.0	2.0	5.0	5.0
H	25.0	12.5	12.5	10.0	10.0	1.0	12.5
H_2	4.0	5.0	5.0	2.0	2.0	1.0	5.0
H_2O	10.0	17.0	5.0	7.0	3.0	1.0	5.0
N	1.0	1.0	10.0	10.0	10.0	1.0	1.0
NO	1.5	3.0	4.0	1.0	1.0	1.0	4.0
N_2	1.5	3.0	4.0	1.0	1.0	2.0	4.0
O	25.0	12.5	12.5	10.0	10.0	1.0	12.5
OH	25.0	12.5	12.5	10.0	10.0	1.0	12.5
O_2	1.5	6.0	11.0	1.0	1.0	25.0	5.0

C. Poorly Characterized Losses, the Energy Release Efficiency

For the purposes of modeling, we have broken down the injector losses into three categories: vaporization, interzonal mixing, and intrazonal mixing.

1. *Vaporization Efficiency*

The vaporization loss is that part of the energy release performance degradation due to either the fuel or oxidizer not completely vaporizing in time to be completely burned. The major obstacle in modeling the vaporization efficiency is obtaining reasonable estimates for the sizes and distributions of the liquid drops. If such estimates are known, then the methods outlined by Priem and Heidmann[20] and Nickerson and Johnson[21] can be applied to subcritical droplet vaporization in one- or two-dimensional flows. Issues related to supercritical droplet vaporization and combustion are addressed in Chapter 7.

2. *Interzonal Losses*

Interzonal variations in mixture ratio are caused by decisions made in the design of the thrust chamber. The most common cause of interzonal striations is the use of a fuel (or oxidizer) film to keep the chamber walls from exceeding

Table 6 Variation in kinetic efficiency with rate data

Reaction	η'_{kin}	η_{kin}
Reference/No changes	0.552	0.9513
$H + H + M = H_2 + M$	0.546	0.9507
$CO + O + M = CO_2 + M$	0.551	0.9512
Change both rates	0.545	0.9505

AIAA The World's Forum for Aerospace Leadership Purchased from American Institute of Aeronautics and Astronautics

their maximum design temperature. Other striations can be caused by the presence of baffles used to suppress acoustic waves. The simplest model for interzonal mixing is a simple mass average of the theoretical *Isp* for each mixture ratio. That is,

$$\eta_{xz} = \sum_{i=1}^{\#\text{zones}} \left[\frac{\dot{m}_{(O/F)_i}}{\dot{m}_t} \right] \cdot Isp[(O/F)_i]/Isp_{\text{th}}(\overline{O/F}) \tag{6}$$

The design values of mass flow for the fuel and oxidizer can be used for initial studies. Cold flow data can supply updated values once testing has begun. Except in rare instances, striations can only be inferred from hot flow heat transfer data.

The moderately complex modeling approach uses the same information as the simple model, but the data are used to generate striation profiles, which are then run though an Euler solver. In such cases the boundary between the striations is a slip line or contact discontinuity. For most cases, the differences between the simple and moderately complex methods are small in terms of performance of the core flow. The effect on the boundary-layer edge condition, however, can be very significant. Also, one must be very careful not to include this loss more than once.

The complex approach can either try to model the injection process or it can use the same data as the moderately complex approach. For the purposes of performance assessment, the use of measured data is probably much more accurate than trying to model the O/F variations directly. However, such modeling can supply a qualitative insight into what is happening in the engine and can be invaluable in understanding problems.

3. *Intrazonal Mixing Loss*

The major problem with modeling intrazonal or micromixing loss is that it cannot be measured directly in either a rocket engine or a reasonable simulation device. The micromixing losses are always inferred by first subtracting out other losses, such as finite rate kinetics, vaporization, and macromixing losses. Both theoretical and empirical micromixing models exist. Spalding,[22] Elghobashi and Pun,[23] and Tamanini[24] assume a two-parameter probability density function to describe the local variation in fuel mixture fraction. The average fuel mixture fraction and other parameters of interest can then be calculated. On the empirical side, C^* correlations based on similar engines are used to estimate the total energy release efficiency loss.

The only recommendation that we can make with respect to modeling the micromixing loss is to use engine-specific empiricisms to estimate the total energy release efficiency loss, subtract out the vaporization and macromixing loss, and then adjust the input enthalpy to match the measured or estimated performance.

V. Approaches

In the United States, the practices used at each engine manufacturer and cognizant analysis organization can vary significantly. However, for engines

AIAA The World's Forum for Aerospace Leadership Purchased from American Institute of Aeronautics and Astronautics

employing standard bell nozzles, the JANNAF procedures as outlined in Ref. 2 are generally followed. These procedures are essentially those outlined in this chapter as the moderately complex modeling approach. That is, the TDK computer program is used to model all of the losses that we have termed "well-characterized losses." The TDK code consists of several modules that compute the *Isp* for a variety of input mixture ratios and enthalpies. The code uses a finite rate kinetics MOC solver to compute the core flow and a finite rate kinetics, finite difference boundary-layer module employing a Cebeci-Smith eddy viscosity turbulence model to compute the boundary-layer loss. The macromixing loss is treated by inputting to the code the O/F and energy content of each striation considered. Gas turbine exhaust dumps can be treated as being injected into either the boundary layer or the core flow. Both cold wall, radiation cooled, and adiabatic wall heat transfer treatments are allowed. Furthermore, the solutions of the core flow and boundary layer can be iterated by displacing the potential wall either inward or outward by the boundary-layer displacement thickness.

One curiosity of the JANNAF procedure is the method of computing the boundary-layer loss. The standard JANNAF equation for the boundary-layer loss is

$$\Delta Isp_{\mathrm{BL}} = 2\pi r \rho_e u_e^2 \theta \cos(\alpha)\left[1 - \frac{\delta^*}{\theta} P_e/\rho_e u_e^2\right]\Big/\dot{m} \tag{7}$$

which is a combination of both the inner and outer solutions applied all at the same time. Kehtarnavaz et al.[25] have extended the derivation of Eq. (7) to thick boundary layers.

The MOC has been shown to be an accurate and efficient flow solver, although there have been many advances in the numerical solutions to rocket nozzle flow. The use of PNS and FNS flow solvers has increased substantially in recent years, especially for very small and very high area ratio engines. Table 7 shows a comparison of results from the TDK and VIPER PNS codes.[26]

Table 7 Comparisons of TDK and PNS nozzle performance predictions

	Isp prediction		
Engine name	TDK/BLM[22]	VIPER[27]	Measured
Adv. Space Engine	473.58	470.20	477.9
Hughes 5 lbf	216.65	218.05	214.52[21]
NASA/LeRC Hi-E	480.31 (458.7)[a]	488.47 (466.49)[a]	468.9
SSME	457.7	455.15	452.6[22]
RL 10	463.03	462.29	458.7
XLR-134	468.68	462.29	——

[a]Corrected for 95.5% measured C^* efficiency.

AIAA The World's Forum for Aerospace Leadership Purchased from American Institute of Aeronautics and Astronautics

The energy release efficiency is usually estimated by using C^* efficiencies from sub- or full-scale testing, from data on similar engines, or backed out from measured *Isp* data. Each engine manufacturer has its own procedures and analytical methods for estimating this loss. Once the loss has been established, it is applied by decreasing the propellant enthalpy until the desired decrease in *Isp* is achieved.

VI. Conclusions

The assessment of thrust chamber performance has been discussed in terms of both the physical phenomena and the modeling of the phenomena. Ideal performance has been defined and deviations from that ideal have also been discussed. Performance losses have been broken down into two categories, well-characterized and poorly characterized losses. The former involve mainly the flow in the nozzle, and the latter are associated with injector performance.

Three levels of modeling, simple, moderately complex, and complex, were discussed. The moderately complex approach has been used successfully in the United States and is more than adequate for performance prediction. The complex approach is recommended only when the fidelity of the input is commensurate with the fidelity of the modeling.

The state of the art in nozzle loss prediction is much better than that of injector performance. There are, however, still issues that need to be resolved. The most important of the issues for nozzle losses is the establishment of an adequate turbulence model for the boundary-layer calculations. A unified model that is applicable for all speed regimes and includes finite rate chemistry is required. In general, the use of empirical data is required to predict the energy release efficiency.

References

[1]Pieper, J. L., "ICRPG Liquid Propellant Thrust Chamber Performance Evaluation Manual," Chemical Propulsion Information Agency, Pub. 178, Sept. 1968.

[2]Evens, S., "JANNAF Rocket Engine Performance Prediction and Evaluation," Chemical Propulsion Information Agency, Pub. 246, April 1975.

[3]Sutton, G. P., *Rocket Propulsion Elements*, 6th ed., Wiley, New York, 1992.

[4]Zucrow, M. J., and Hoffman, J. D., *Gas Dynamics*, Wiley, New York, 1976.

[5]Gordon, S., and McBride, B. J., "Computer Program for Calculation of Complex Chemical Equilibrium Compositions, Rocket Performance, Incident and Reflected Shocks, and Chapman Jouguet Detonations," NASA SP-273, 1971.

[6]Gordon, S., and McBride, B. J., "Computer Program for Calculation of Complex Chemical Equilibrium Compositions and Applications," NASA RP-1311, Oct. 1994.

[7]Coats, D. E., Berker, D. R., and Kawasaki, A. H., "Boundary Layer Loss Models in Nozzle Performance Predictions," Chemical Propulsion Information Agency, Pub. 529, Oct. 1989.

[8]Cebeci, T., and Smith, A. M. O., *Analysis of Turbulent Boundary Layers*, Academic Press, New York, 1974.

[9]Hall, I. M., "Transonic Flow in Two-Dimensional and Axially-Symmetric Nozzles," *Quarterly Journal of Mechanics and Applied Mechanics*, Vol. XV, Pt. 4, 1962, pp. 487–508.

[10]Kliegel, J. R., and Levine, J. N., "Transonic Flow in Small Throat Radius of Curvature Nozzles," *AIAA Journal*, Vol. 7, No. 7, July 1969, pp. 1375–1378.

AIAA The World's Forum for Aerospace Leadership Purchased from American Institute of Aeronautics and Astronautics

[11]Weingold, H. D., "The ICRPG Turbulent Boundary Layer (TBL) Reference Program," ICRPG Perf. Std. Working Group, Pratt and Whitney Aircraft, East Hartford, CT, July 1968.

[12]Kliegel, J. R., Nickerson, G. R., Frey, H. M., Quan, V., and Melde, J. E., "Two-Dimensional Kinetics Nozzle Analysis Computer Program-TDK," ICRPG Performance Standardization Working Group, Dynamic Science Corp., Monrovia, CA, July 1968.

[13]Kushida, R., Hermal, J., Apfel, S., and Zydowicy, M., "Performance of High-Area Ratio Nozzle for a Small Rocker Thruster," *Journal of Propulsion and Power*, Vol. 3, No. 4, p. 329.

[14]Nickerson, G. R., Berker, D. R., Coats, D. E., and Dunn, S. S., "Two-Dimensional Kinetics (TDK) Nozzle Performance Computer Program Volume II, Users Manual," Software and Engineering Associates, Inc., Contract NAS8-39048, Carson City, NV, March 1993.

[15]Baulch, D. L., Drysdale, D. D., Horne, D. G., and Lloyd, A. C., *Evaluated Kinetic Data for High Temperature Reactions, Vol. II Homogeneous Gas Phase Reactions for the H_2-O_2-N_2 System*, CRC Press, Cleveland, OH, 1972.

[16]Baulch, D. L., Drysdale, D. D., Duxbury, J., and Grant, S., *Evaluated Kinetic Data for High Temperature Reactions, Vol. III Homogeneous Gas Phase Reactions of the O_2-O_3 System, The CO-O_2-H_2 System, and of Sulfur-Containing Species*, Butterworths, London, 1976.

[17]Baulch, D. L., Drysdale, D. D., Horne, D. G., and Lloyd, A. C., *Evaluated Kinetic Data for High Temperature Reactions, Vol. II Homogeneous Gas Phase Reactions for the H_2-O_2-N_2 System*, CRC Press, Cleveland, OH, 1973.

[18]Jensen, D. E. and Jones, G. A. "Reaction Rate Coefficients for Flame Calculations," *Combustion and Flame*, Vol. 32, 1978, pp. 1–34.

[19]Kushida, R., "Revision of CPIA 246, Section 6.2, Reaction Rate Data," Jet Propulsion Lab., JPL 383CR-76-211, Pasadena, CA, March 1976.

[20]Priem, R. J., and Heidmann, M. F., "Propellant Vaporization as a Design Criterion for Rocket-Engine Combustion Chambers," NASA TR R-67, 1964.

[21]Nickerson, G. R., and Johnson, C. W., "SCAP-Spray Combustion Analysis Program," Phillips Lab., PL-TR-94-3032, Edwards AFB, CA, Aug. 1993.

[22]Spalding, D. B., "Concentration Fluctuations in a Round Turbulent Jet," *Chemical Engineering Science*, Vol. 26, 95, 1971.

[23]Elghobashi, S. E., and Pun, W. M., "A Theoretical and Experimental Study of Turbulent Diffusion Flames in Cylindrical Furnaces," *Fifteenth Symposium (International) on Combustion*, Combustion Inst., Pittsburgh, PA, 1975, p. 1353.

[24]Tamanini, F., "On the Numerical Prediction of Turbulent Diffusion Flames," Eastern States Section/Combustion Inst., Pittsburgh, PA, April 1976.

[25]Kehtarnavaz, H., Coats, D. E., and Dang, A. L., "Viscous Loss Assessment in Rocket Engines," *Journal of Propulsion and Power*, Vol. 6, No. 6, Nov.–Dec. 1990, pp. 713–717.

[26]Kawasaki, A. H., Dunn, S. S., Coats, D. E., Nickerson, G. R., and Berker, D. R., "Viscous Interaction Performance Evaluation Routine for Two-Phase Nozzle Flows with Finite Rate Chemistry, VIPER 3.0, Volume I: Computer Reference Manual," Software and Engineering Associates, Inc., Contract F29601-91-C-0099, Carson City, NV, May 1994.

[27]Coats, D. E., Berker, D. R., and Dunn, S. S., "Boundary Layer Study," U.S. Air Force Astronomical Lab. AL-TR-90-040, Contract F04611-86-C-0055, Nov. 1990.

AIAA The World's Forum for Aerospace Leadership Purchased from American Institute of Aeronautics and Astronautics

Color reproductions for Chapter 12

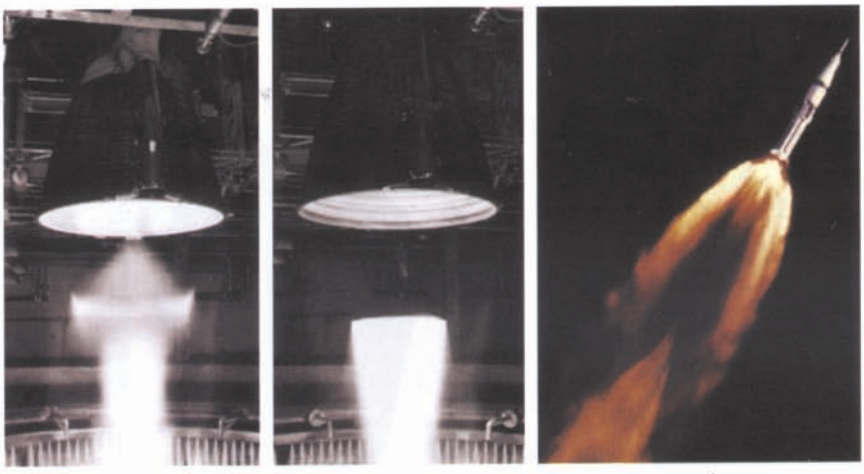

a) b) c)

Fig. 2 Rocket nozzle flowfield during off-design operation: a) overexpanded flow with cap-shock pattern Vulcain engine, b) overexpanded flow with Mach disk Vulcain engine, and c) underexpanded flow Saturn-1B, Apollo-7 (photographs Dasa, SNECMA, NASA).

GOX/GH_2 thrust chamber operating at 40% power level featuring free shock separation

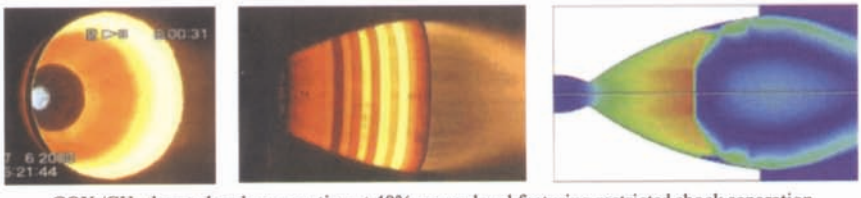

GOX/GH_2 thrust chamber operating at 40% power level featuring restricted shock separation

Fig. 6 Hot-firing test with GOX/GH_2 thrust chamber designed for 40-kN vacuum thrust level at 40% power level featuring free shock separation (top figures) and restricted shock separation (bottom figures). CFD results for flow visualization (Mach number distribution, from blue to red for increasing Mach number).

AIAA The World's Forum for Aerospace Leadership Purchased from American Institute of Aeronautics and Astronautics

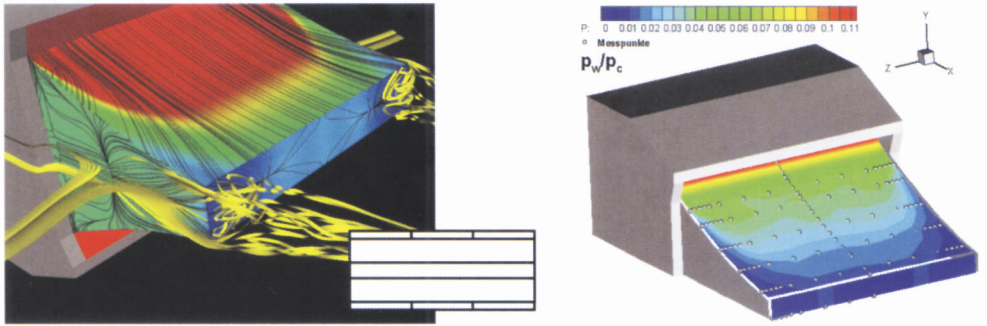

Linear plug nozzle without side-fences, numerical (left) and experimental results (right).

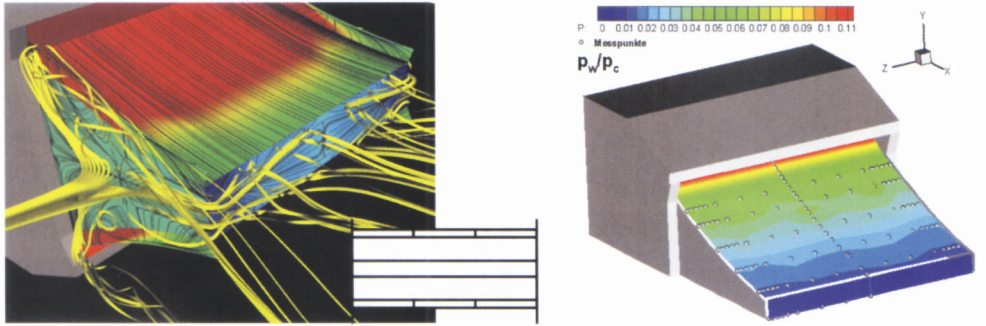

Linear plug nozzle with side-fences, numerical (left) and experimental results (right).

Fig. 19 Flow phenomena for a linear plug nozzle without side fences (top figure) and with side fences (bottom figure): numerical results, Mach number distribution and streamlines (left, from red to blue for increasing Mach number), and experimental results, pressure ratio p_w/p_c distribution (right, from red to blue for increasing pressure ratio). (CFD images courtesy of NASA Marshall Space Flight Center; see also Ref. 56.)

AIAA The World's Forum for Aerospace Leadership Purchased from American Institute of Aeronautics and Astronautics

Color reproductions for Chapter 14

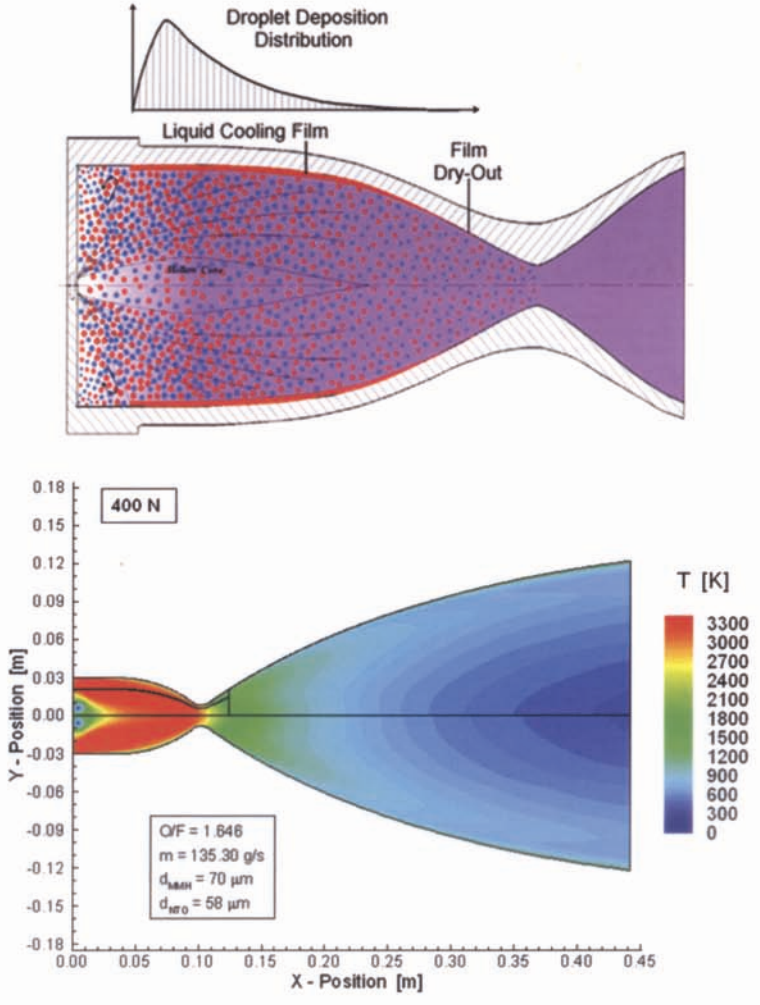

Fig. 3 Sketch of a liquid film cooled 400-N apogee thruster illustrating the droplet flowfield and annular cooling film evolution (top) and temperature contours of a corresponding CFD simulation (bottom).

AIAA The World's Forum for Aerospace Leadership Purchased from American Institute of Aeronautics and Astronautics

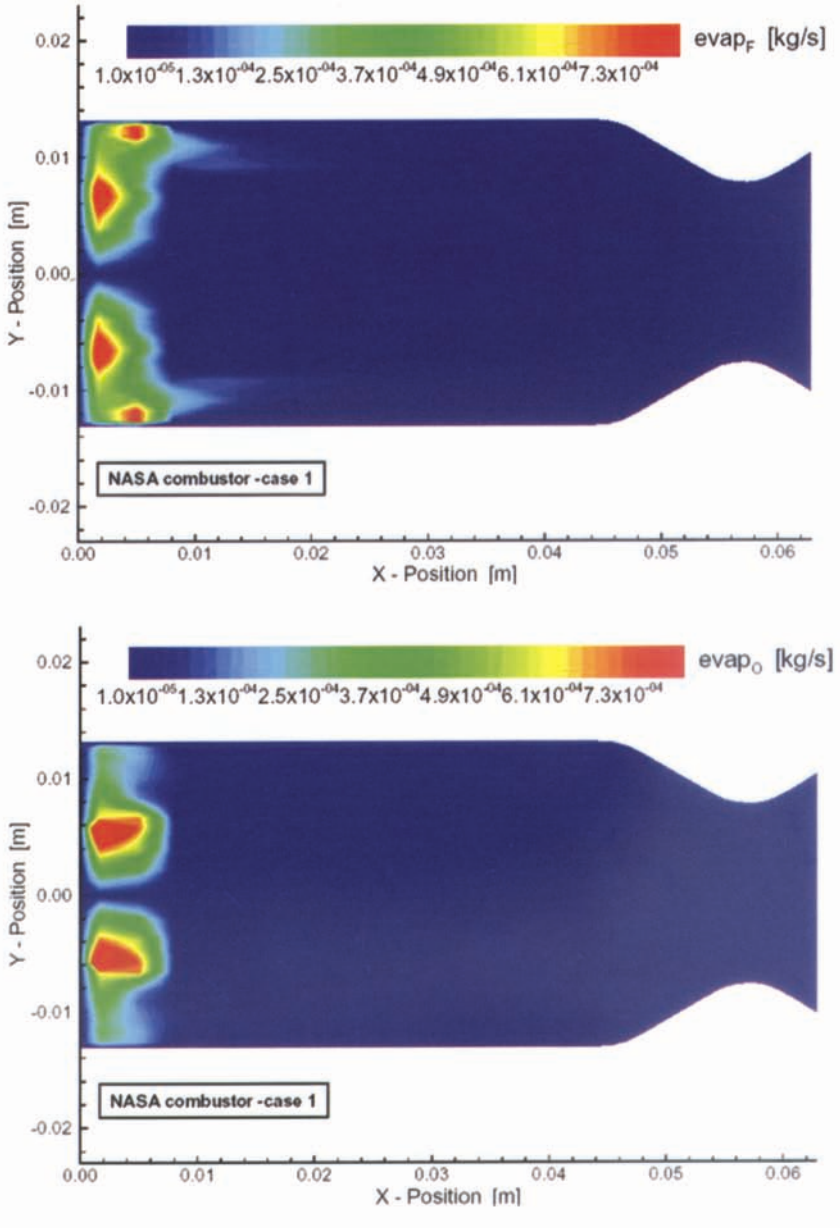

Fig. 4 Calculated hydrazine (top) and NTO (bottom) evaporation rates for combustor test case 1 (Ref. 19).

AIAA The World's Forum for Aerospace Leadership Purchased from American Institute of Aeronautics and Astronautics

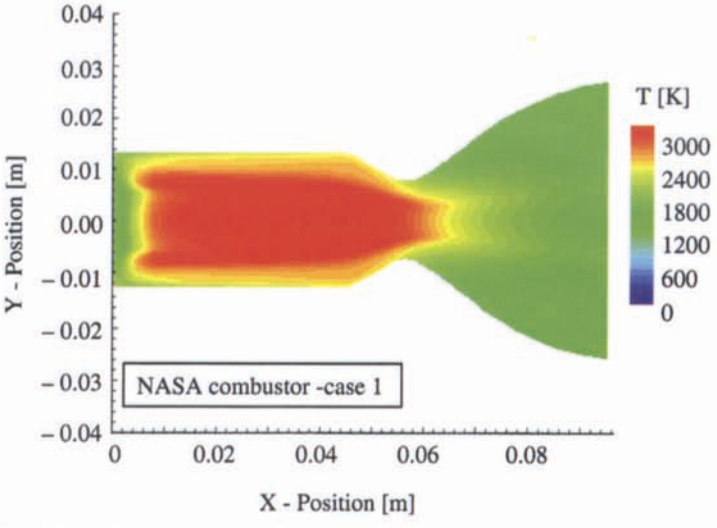

Fig. 5 Calculated gas temperature contours for combustor and nozzle test case 1 (Ref. 19).

AIAA The World's Forum for Aerospace Leadership Purchased from American Institute of Aeronautics and Astronautics

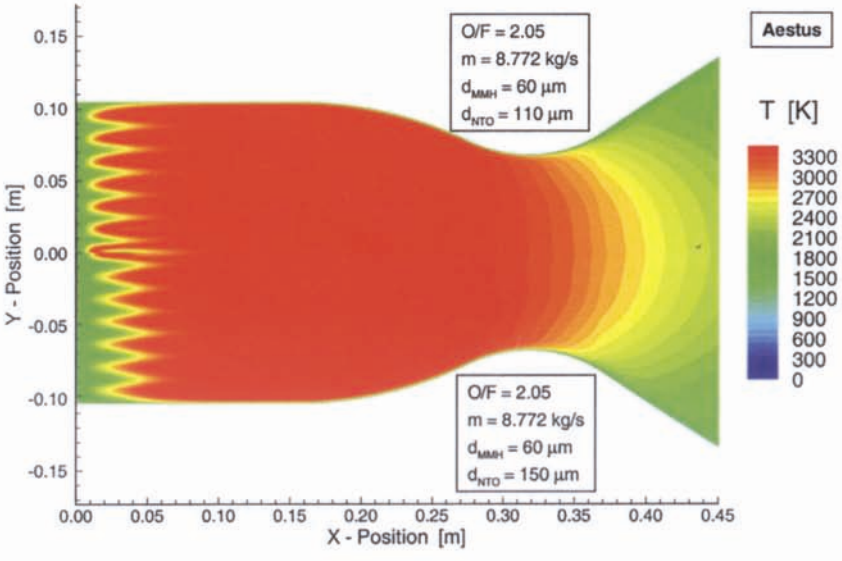

Aestus/OMS Post Test Condition

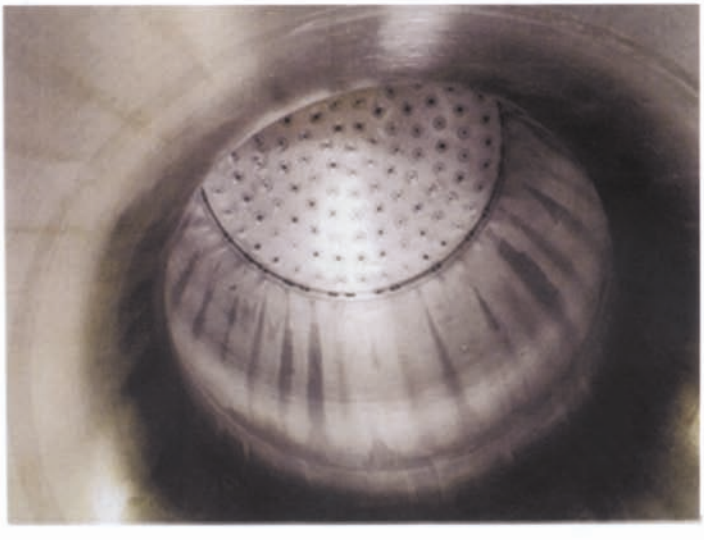

Fig. 8 Comparison of computational temperature stratifications close to the injector plate resulting from two different oxidizer spray patterns: upper half $D_{NTO} = 100\ \mu m$, lower half $D_{NTO} = 150\ \mu m$ (top), and photography taken from tested Aestus hardware illustrating the effect of temperature stratification (bottom).

AIAA The World's Forum for Aerospace Leadership Purchased from American Institute of Aeronautics and Astronautics

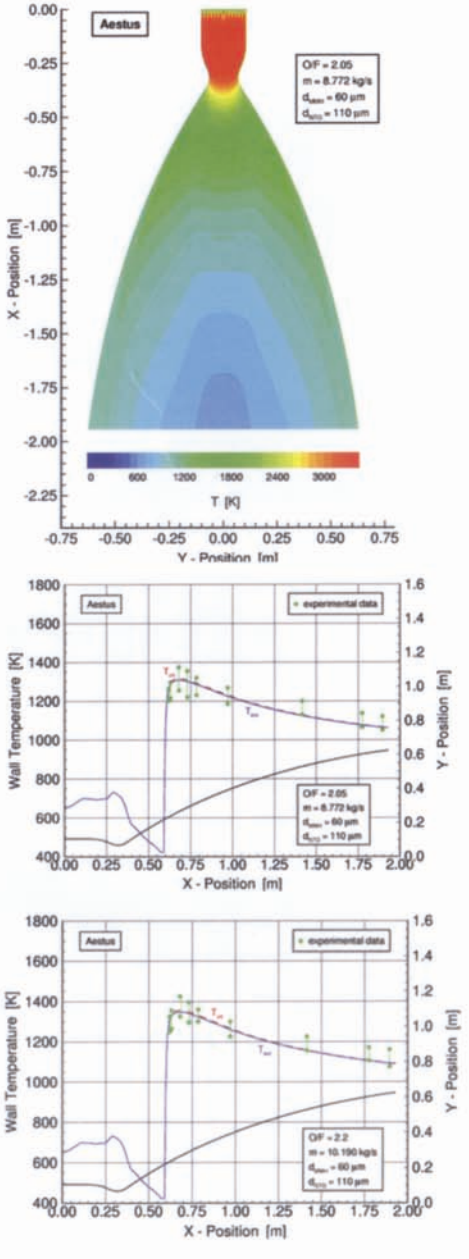

Fig. 10 Temperature contours predicted for the reference load point *R* (top) and external and internal wall temperature distribution for load point *R* (middle) and *Q5′* (bottom).

AIAA The World's Forum for Aerospace Leadership Purchased from American Institute of Aeronautics and Astronautics

Color reproductions for Chapter 15

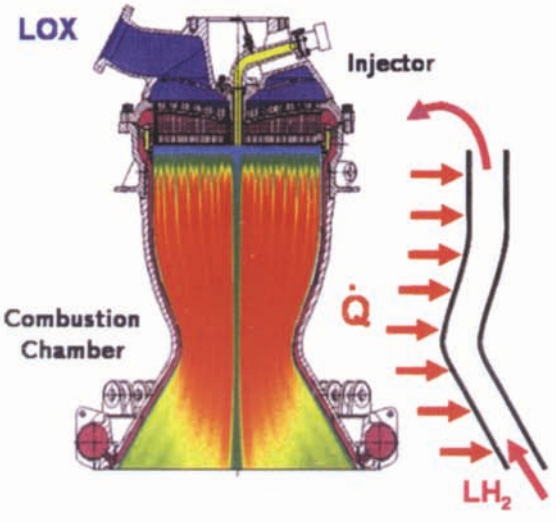

Fig. 2 Flow schematic for regeneratively cooled combustion chamber.

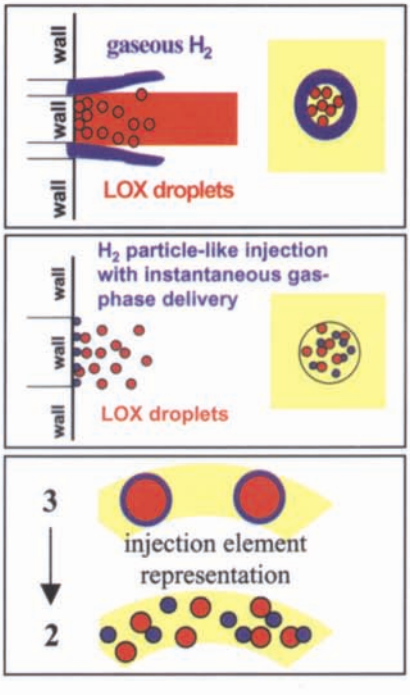

Fig. 4 Schematic of non-premixed, coaxial LOX/H_2 injection employing a liquid jet cone (top), well-premixed injection (center), and the principal representation of an injection element row through an axisymmetrical treatment (bottom).

AIAA The World's Forum for Aerospace Leadership Purchased from American Institute of Aeronautics and Astronautics

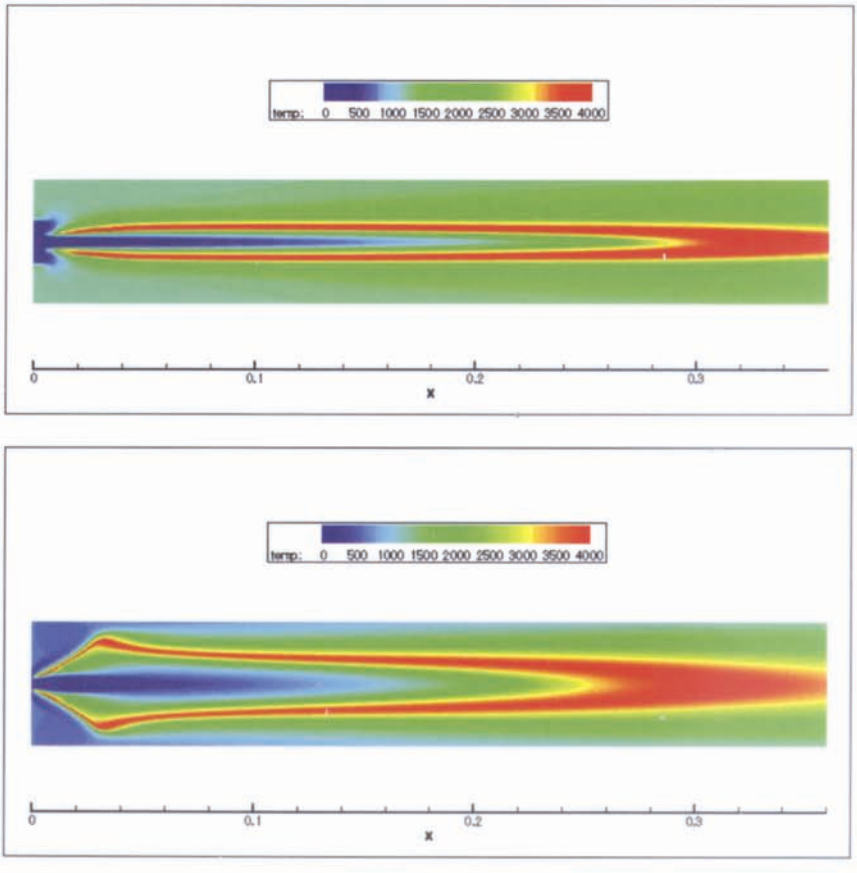

Fig. 5 Temperature distribution for single-element combustor test case ($P_c = 10$ bar) employing a standard grid resolution applicable to a multi-element injection system (top) and a strongly refined grid resolution (bottom).

AIAA The World's Forum for Aerospace Leadership Purchased from American Institute of Aeronautics and Astronautics

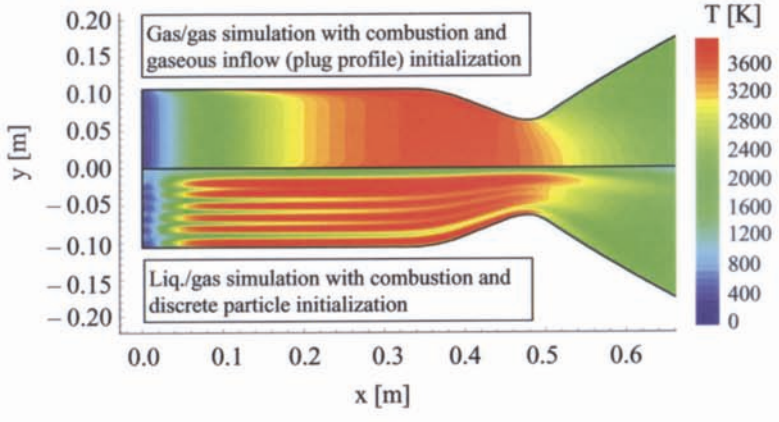

Fig. 9 Hot gas temperature distribution inside a combustion chamber obtained for a gas/gas simulation with plug-inflow profile (upper half) and liquid/gas discrete particle (lower half) initialization, both with turbulent combustion and prescribed wall temperature boundary conditions (boundary-layer model: logarithmic wall functions).

AIAA The World's Forum for Aerospace Leadership Purchased from American Institute of Aeronautics and Astronautics

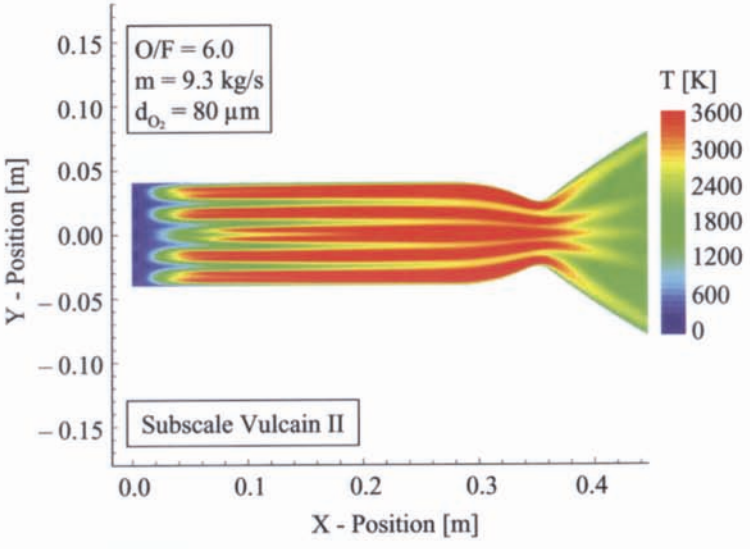

Fig. 11 LOX/H_2 temperature distribution and flowfield stratification inside subscale chamber employing the discrete particle initialization method (top); "footprints" of near-wall injection elements observed on divergent part of nozzle throat wall (bottom) during hot firing; operational load point: $P_c = 100$ bar; $O/F = 6$.

AIAA The World's Forum for Aerospace Leadership Purchased from American Institute of Aeronautics and Astronautics

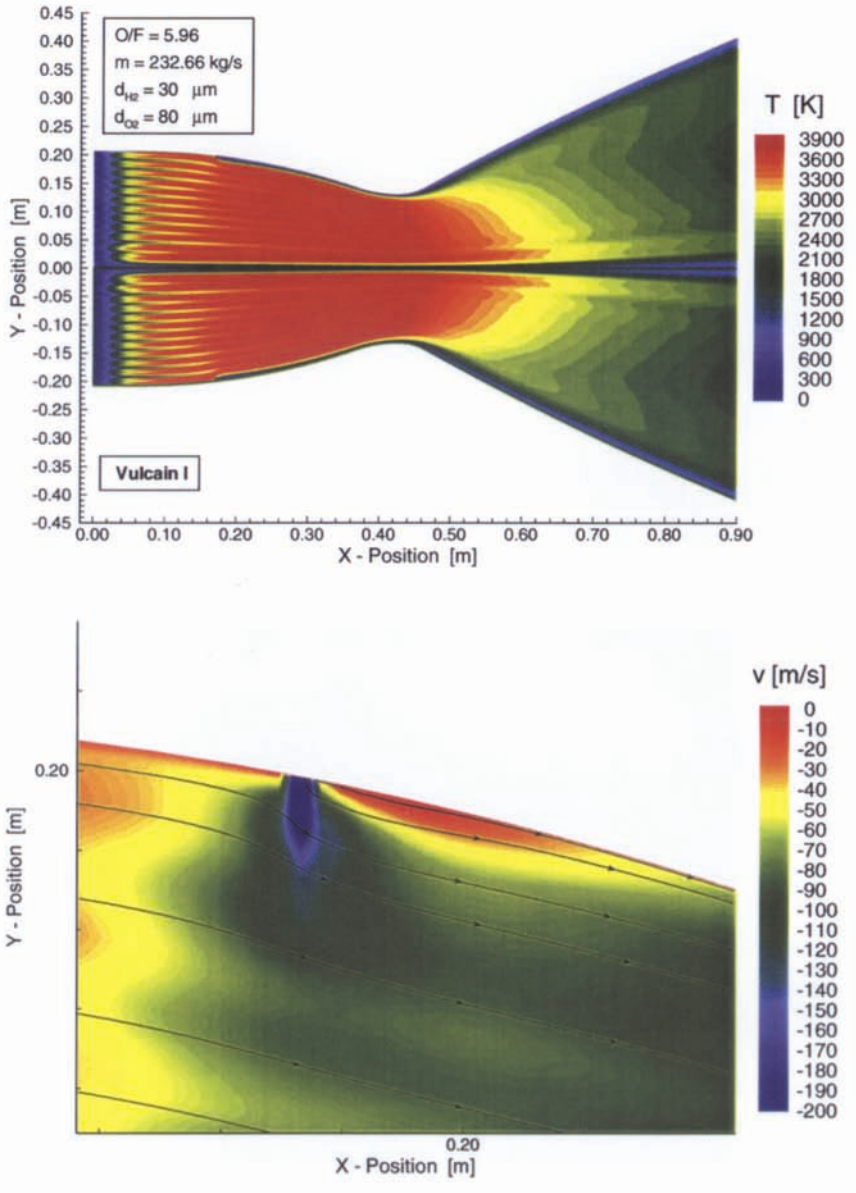

Fig. 14 Temperature distribution inside a rocket combustion chamber with an artificial crack 170 mm downstream of the injector (top), and local velocity profile with streamlines around the crack (bottom).

AIAA The World's Forum for Aerospace Leadership Purchased from American Institute of Aeronautics and Astronautics

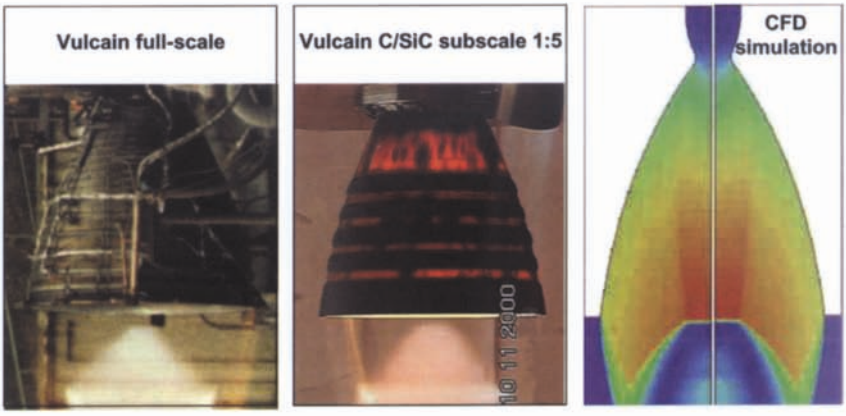

Fig. 18 Comparison of Vulcain-type full-flowing nozzles at nearly identical operational conditions: full-scale (left), long C/SiC subscale (middle), and numerical simulation for full-scale (right)).

AIAA The World's Forum for Aerospace Leadership Purchased from American Institute of Aeronautics and Astronautics

Color reproductions for Chapter 20

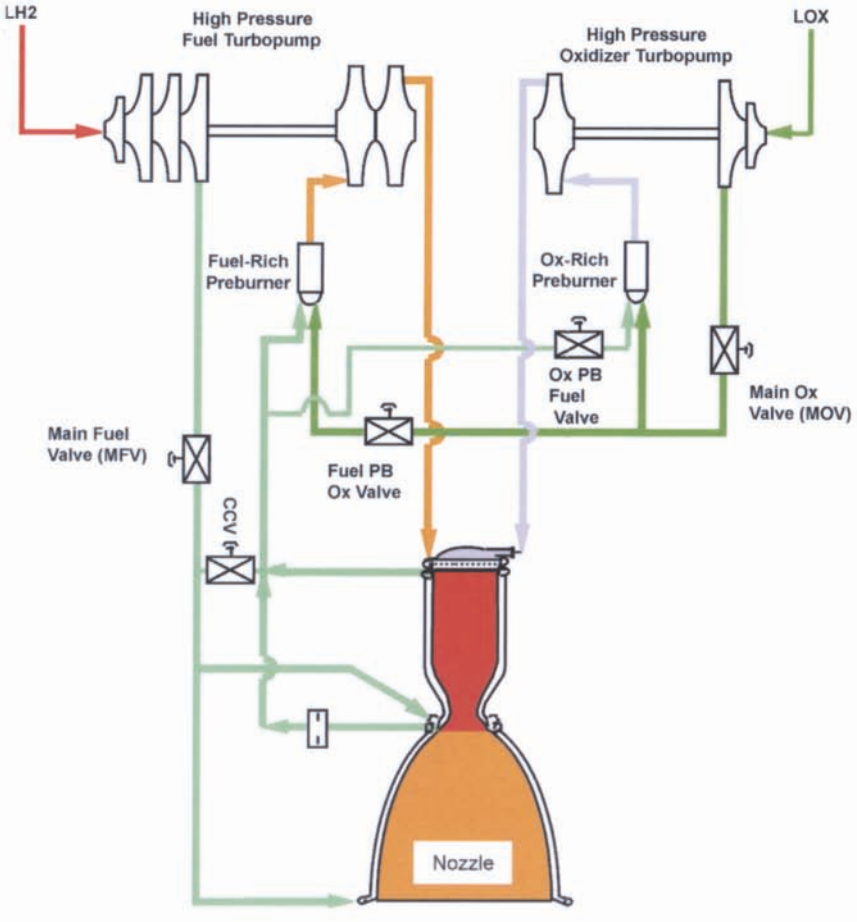

Fig. 1 Full-flow staged combustion booster engine schematic.

AIAA The World's Forum for Aerospace Leadership Purchased from American Institute of Aeronautics and Astronautics

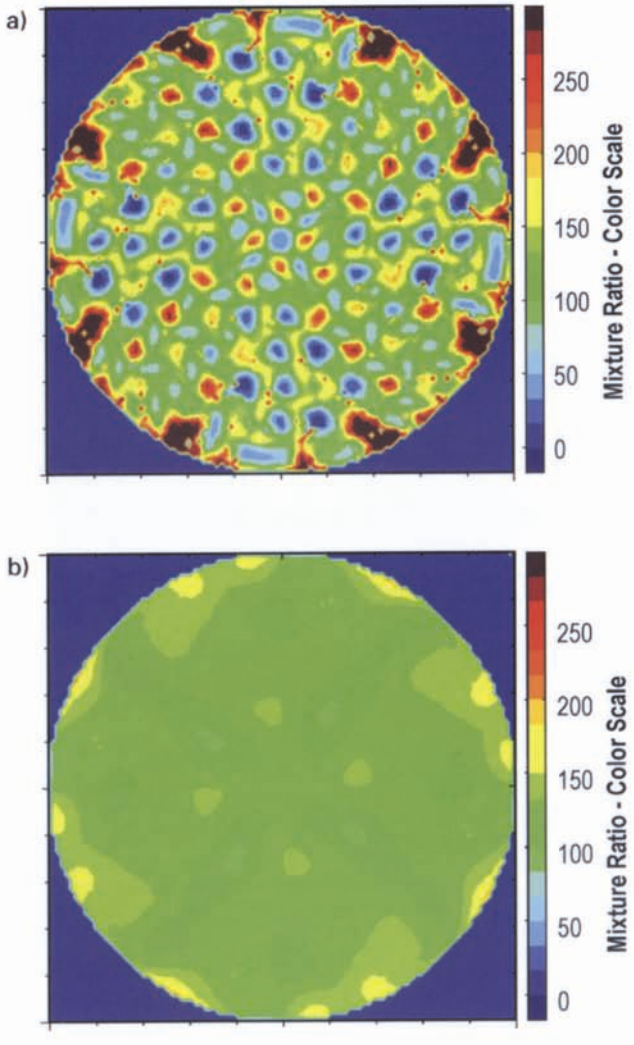

Fig. 7 Predicted mixture ratio distribution at a) 1.27 cm and b) 3.81 cm from the injector for a P_c of 24.1 MPa and *MR* of 135.

AIAA The World's Forum for Aerospace Leadership Purchased from American Institute of Aeronautics and Astronautics

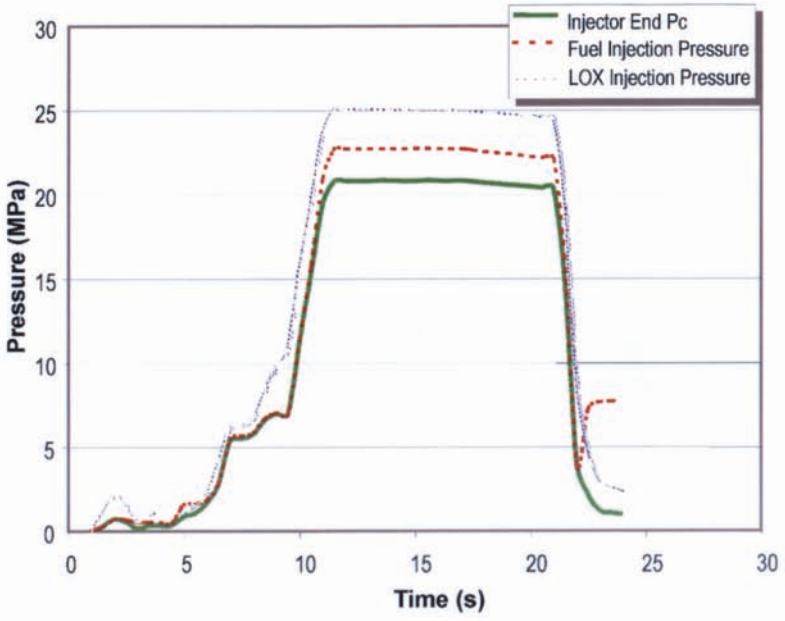

Fig. 11 Test 034 injection and chamber pressures.

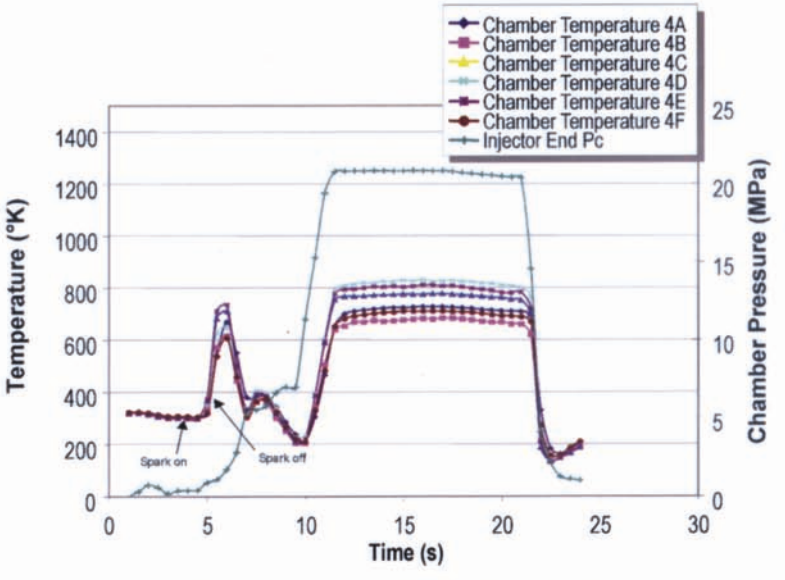

Fig. 12 Test 034 temperature rake data.